Desalination and Water Treatment
www.deswater.com
doi: 10.1080/19443994.2014.922443

55 (2015) 1096–1104
July

Taylor & Francis
Taylor & Francis Group

Investigation of the photocatalytic activity of supported ZnO–TiO_2 on clinoptilolite nano-particles towards photodegradation of wastewater-contained phenol

Alireza Nezamzadeh-Ejhieh[a,*], Mohsen Bahrami[b]

[a]*Department of Chemistry, Shahreza Branch, Islamic Azad University, P.O. Box 311-86145, Shahreza, Isfahan, Iran, Tel. +98 321 3292515; Fax: +98 321 3291018; email: arnezamzadeh@iaush.ac.ir*
[b]*Young Researchers Club, Shahreza Branch, Islamic Azad University, Shahreza, Iran, Tel. +98 321 3292104; Fax: +98 321 3291018; email: sofalineh@gmail.com*

Received 8 November 2013; Accepted 1 May 2014

ABSTRACT

Photodegradation of a phenol wastewater sample with ZnO–TiO_2 supported on nano-clinoptilolite particles (NCP) was studied. NCP were obtained by planetary ball mill. The proposed catalyst was obtained via ion exchanging of NCP with $Zn(NO_3)_2 \cdot 6H_2O$ and $C_4H_{10}N_2O_{10}Ti \cdot H_2O$ (0.2 M) aqueous solutions for 12 h followed by calcination at 450°C for 12 h. XRD, FT-IR, and TEM were used for characterization of samples. The best degradation efficiency was related to the catalyst containing both ZnO and TiO_2. The optimum values were 0.1 g L^{-1} of photocatalyst, 100 times diluted wastewater solution, and pH of 3.0 in photodegradation studies.

Keywords: Advanced oxidation processes; Phenol; Nano-zeolite; Clinoptilolite; Wastewater; ZnO; TiO_2

1. Introduction

Phenols are one of the most important pollutants in textile industry wastewaters. Unfortunately, many conventional methods for removing the phenolic pollutants, such as adsorption [1], chemical coagulation and biological treatments [2,3], solvent extraction [4], and pervaporation using membranes [5], do not have sufficient removal efficiency [6]. Recently, advanced oxidation processes (AOPs), based on the production of highly reactive hydroxyl radicals, have been proposed as an efficient method for the removal of phenolic compounds and other pollutants [7–9]. Heterogeneous photocatalysis based on the semiconductors is the most famous AOP in the recent decades in which irradiating the semiconductor by photons with sufficient energy with respect to bang gap energy of semiconductor produces electron-hole pairs. The produced e-holes can generate reactive hydroxyl or super oxide radicals by reaction of e-hole with water and dissolved molecular oxygen, which can destroy different organic pollutants to smaller fragments and finally to water and carbon dioxide [7–10]. Among various semiconductors, ZnO and TiO_2 have been widely used in photodegradation experiments [11–14]. Based on the literature, supporting the semiconductors on suitable supports such as zeolites prevents the formation of aggregation and also electron-hole recombination, where both increase the degradation efficiency of the supported semiconductors [15–17].

---

*Corresponding author.

Phenol as one of the most important environmental pollutant is quite toxic, even its low concentration (5–25 mg L^{-1}) is lethal to fish, and at concentrations of about 0.5 mg L^{-1} can cause unpleasant taste in drinking water. Several industries including petroleum refineries, olive oil mills, petrochemical plants, and oil-field activities generate waste streams containing significant amount of phenol and its derivatives. Hence, in order to prevent health and environmental hazards by phenol and phenolic compounds, phenol-containing wastewater should be pre-treated for reducing the phenol content prior to discharge to the environment [18–20]. The purpose of this work is to study the photodegradation process in order to remove phenol from a real sample of wastewater by using modified clinoptilolite nano-particles by ZnO and TiO_2 ($ZnO–TiO_2/NCP$) semiconductors. In general, coupling of semiconductors with different energy levels prevents electron-hole recombination as a desirable phenomenon in the photodegradation processes and significantly enhances the efficiency of the method [21]. The effect of some key operating factors on the photodegradation efficiency was studied and the results were fitted to first-order kinetic model for the calculation of rate constants.

2. Experimental

2.1. Materials

The natural zeolite clinoptilolite tuffs (CP), belong to the Semnan region in the northeast of Iran, were prepared from Afrand Touska Company (Isfahan-Iran). $Zn(NO_3)_2 \cdot 6H_2O$, $C_4H_{10}N_2O_{10}Ti \cdot H_2O$ and other used analytical grade chemicals were purchased from Aldrich or Merck. Distilled water was used throughout the experiments. The pH of solutions was appropriately adjusted with sodium hydroxide or hydrochloric acid solution. The used wastewater sample was prepared from Toka Co., which is one of the companies in Mobarakeh industrial town in the southwest of Isfahan-Iran, and it was used after simple filtration.

2.2. Preparation of nano-particles and catalyst

The natural clinoptilolite tuffs were mechanically pretreated, by crushing in an agate mortar and sieving in analytical sieves, for separating the particles ≤100 μm. The obtained powder was used to prepare nano-particles of zeolite using a planetary ball mill (PM100; Retsch Corporation). The particles smaller than 100 μm were used in dry milling during 6 h. All the tests were done in a 250 mL stainless steel jar with protective jacket of polymer. Zirconium oxide balls of 20 and 3 mm were used for dry and wet millings; respectively. In order to remove magnetic impurities, aqueous suspension of the powder was magnetically stirred for 8 h; and at definite time intervals (15 min), the magnet gave out impurities and the adsorbed magnetic particles were removed. After getting a relative confidence for removing magnetic impurities, for removing water soluble impurities and also to reach completer removing of magnetic impurities the suspension was refluxed at 70℃ for 24 h under magnetic stirring. The water content of the suspension was renewed every 8 h to reach complete purification. Finally, the suspension was centrifuged and the solid material was dried at 100℃ for 3 h.

Then 25 mL of aqueous solution $C_4H_{10}N_2O_{10}$-$Ti \cdot H_2O$ with concentration of 0.4 M and 25 mL 0.4 M Zn^{2+} aqueous solution with the same concentration was added to 2 g NCP powder. The suspension was shaken at room temperature for 24 h and then centrifuged and the residue (Zn–Ti–NCP) was washed with copious water and dried at room temperature. The obtained solid was calcined at 450℃ for 12 h to produce the $ZnO–TiO_2$ nano-clinoptilolite catalyst ($ZnO–TiO_2/NCP$).

2.3. Photocatalytic degradation experiments

The photodegradation experiments of wastewater were conducted with Hg lamp (35 W) as irradiation source. The surface adsorption extent of the pollutants on the surface of the used photocatalyst was studied in a dark condition. An appropriate amount of the photocatalyst was added to a 20 mL adequate diluted wastewater to obtain the desired dose of the catalyst (e.g. to 0.1 g L^{-1} catalyst dose as optimum value). The suspension was shaken in the regular time intervals and centrifuged. The amount of adsorbed pollutants was measured spectrophotometrically. To eliminate the surface adsorption effect in the removal of pollutant, prior to photocatalytic experiments, the suspensions were magnetically stirred for 30 min. The direct photolysis of the same mixture was also studied by subjecting it under UV irradiation in the absence of the photocatalyst.

To study the photodegradation of the proposed wastewater sample, 20 mL of 100 times diluted sample containing 0.1 g L^{-1} of the photocatalyst was constructed in a cylindrical Pyrex-glass cell (5 cm inside diameter and 10 cm height) as a reactor. The suspensions were irradiated with a medium pressure Hg lamp (35 W, Philips) which was positioned above the reactor in a distance of 30 cm with respect to the sample cell. During the irradiation, the suspension was sampled out at the regular time intervals and centrifuged to remove any suspended solid particles. Based on the absorption spectrum of the clear solution, the degradation extent was calculated in terms of the change in the absorbance at the $\lambda_{\max} = 270$ nm. The degradation extent was calculated by the following equation:

$$\begin{aligned}\text{Degradation } \% &= [(C_0 - C_t)/C_0] \times 100 \\ &= [(A_0 - A_t)/A_0] \times 100 \end{aligned} \quad (1)$$

where C_0, C_t, A_0, and A_t are the initial concentration of the pollutant, contaminant concentration after irradiation time t, initial absorbance, and final absorbance of the sample after irradiation time t, respectively [22,23].

2.4. Characterization

A planetary ball mill (PM100; Retsch Corporation) was used to prepare nano-particles of the natural zeolite. The Fourier transformation infrared spectra (FT-IR) were recorded at room temperature using a Nicolet single beam FT-IR (Impact 400D) spectrophotometer and KBr pellets. The X-ray diffraction pattern of samples was prepared using a Bruker diffractometer (D8 Adyance) with Ni-filtered copper radiation ($K_\alpha = 1.5406$ Å) in the 2θ range of 5–60˚. Average crystallite sizes of the prepared particles were calculated by Scherrer equation. TEM images were recorded Transmission electron microscopy (CM_{10}, Philips). The diffuse reflectance spectroscopic (DRS) studies were carried out using Shimadzu UV 3600 equipped with an integrating sphere. $BaSO_4$ was used as the reference material. Before this study, all samples were heated at 250˚C for 3 h. The absorption spectra were registered on a double-beam spectrophotometer (Carry 100 Scan) in quartz cells of 1 cm optical path length and the absorbance of samples was measured in the wavelength range of 190–900 nm. The degradation extent the pollutant was determined using the measured absorbance of the cleaned sample (by centrifuging the sample) before and after the irradiation process of samples. Measurements of total organic carbon (TOC) were performed by TOC analyzer (Shimadzu TOC-VCSN). An atomic absorption spectrometer, Perkin Elmer AAnalyst 300, was used for determination of the zinc and titanium content of the catalysts (by digesting the catalysts in a mixture of $HNO_3 + HClO_4 + HF$).

To determine the pH of point of zero charge, pH_{pzc}, some experiments were carried out as follows [24]: The pH of a series of 50 mL 0.01 M NaCl solutions was adjusted to a value between 2 and 12 by adding HCl 0.1 M or NaOH 0.1 M solution in closed Erlenmeyer flasks. Before adjusting the pH, all solutions were degassed by purging N_2 gas to remove dissolved CO_2. The pH of these solutions was recorded as the initial pHs (pH_I). Then, 0.2 g of the NCP or $ZnO–TiO_2/NCP$ sample was added and the final pH (pH_F) was measured after 48 h agitation of the suspensions at room temperature. Finally, the plot of pH_F vs. pH_I was constructed. The pH_{pzc} is the point where the line pH_I vs. pH_I crosses the curve pH_F *vs.* pH_I. On the other hand, to have a straight line which crosses the original curve, the pH_I should be plotted vs. pH_I.

3. Results and discussion

3.1. Characterization studies

3.1.1. XRD and TEM results

Fig. 1(A) shows the XRD patterns of raw NCP, TiO_2 supported nano-clinoptilolite (TiO_2/NCP), ZnO supported nano-clinoptilolite (ZnO/NCP), and $ZnO–TiO_2$ supported nano-clinoptilolite ($ZnO–TiO_2$ /NCP) samples at 2θ-range from 3˚ to 80˚. The pattern (a) belongs to the XRD pattern of raw NCP, which shows characteristics reflection lines at 2θ values of 10.0˚, 11.2˚, 13.3˚, 17.5˚, 18.3˚, 22.2˚, 26.7˚, 30.5˚, and 32.1˚. The observed reflection peaks in Fig. 1(A) can be indexed to clinoptilolite crystalline structure data in the library of the instrument [JCPDS No. 39-1383], which also show good agreement with the XRD data of clinoptilolite in the literature [25]. This confirms that the used zeolite tuff includes clinoptilolite phase as a major component. Based on the XRD results, slight amounts of quartz (3.5%) and cristobalite (7.8%) were also present in the used tuff. Presence of new peaks at 2θ of 32.8˚ and 35.8˚ in the XRD pattern of TiO_2/NCP (Fig. 1(A–B)) shows loading of TiO_2 onto the zeolite framework [26,27]. These agree with the XRD data of TiO_2 (JCPDS No. 21-1276 and 29-1360). Pattern (c) shows new reflection lines were located at 28.5˚, 30.7˚, 33.5˚, and 37.1˚, which are in agreement with the JCPDS file for ZnO (JCPDS 36-1451) and can be indexed as a wurtzite hexagonal phase of ZnO. This in turn confirms sufficient loading of ZnO particles onto the zeolite framework. In addition, the reflection lines of ZnO and TiO_2 are present in the XRD pattern of combined $ZnO–TiO_2/NCP$ at 2θ values of 33.5 and 37.1 (for ZnO) and 35.8 for (TiO_2). However, the crystallinity and hence the intensity of all nano-samples were decreased with respect to the original parent clinoptilolite. Our results are in agreement with the literature [28] which showed that the loss in the crystallinity during the ball milling

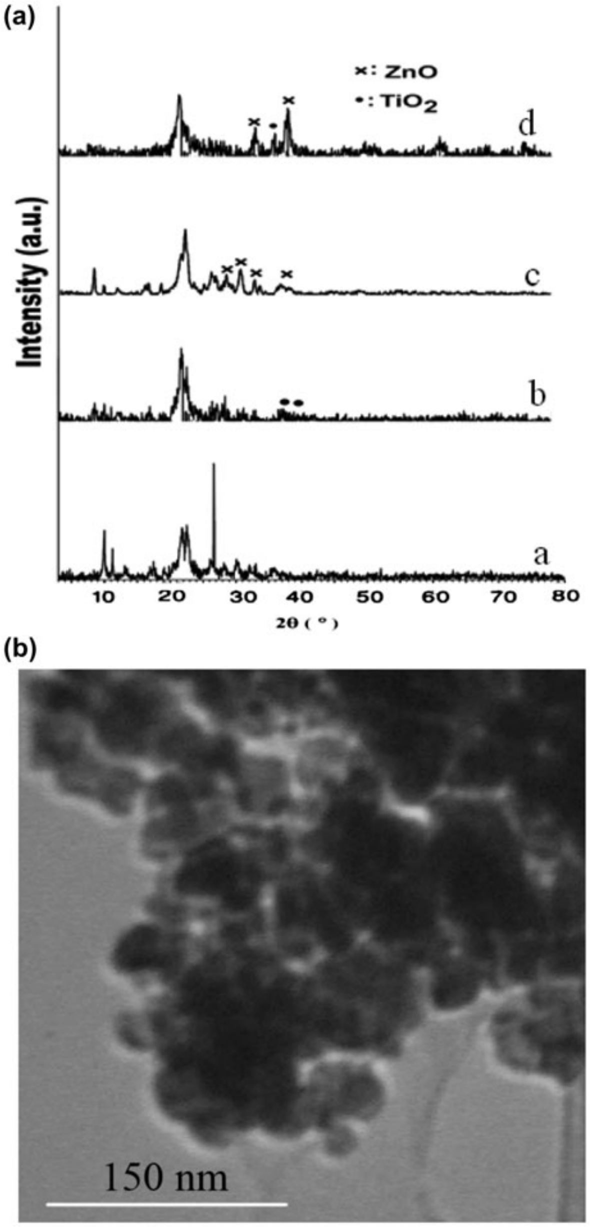

Fig. 1. (A): XRD patterns of (a) NCP, (b) TiO_2/NCP, (c) ZnO/NCP, (d) ZnO–TiO_2/NCP; (B): TEM image of ZnO–TiO_2/NCP sample.

process of natural clinoptilolite depends on the used conditions including dry and wet milling durations, rotational speed, balls to powder ratio, and water to powder ratio. XRD patterns also show that there are no considerable shifts at the peaks position of the raw and treated samples. Decrease in the intensity of the calcined samples may be explained by the fact that although the crystal structure of the clinoptilolite does not destroy during the calcination, some amorphous structure maybe formed (such as amorphous or crystallized ZnO or TiO_2 due to aggregation of ZnO or TiO_2 particles on the NCP surface) [29]. Changing in the peak intensities can also be considered due to presence or interaction of cations and semiconductors with the matrix structure [30].

Presence of the broad lines in the XRD pattern of the prepared samples agrees with the formation of nano-particles during the ball milling process. So, we determined the average size of the samples using β, the excess of width line of the diffraction peak in radians, and θ, the Bragg angle in degrees, and using Scherrer equation [8,31] as:

$$d = 0.9\lambda/\beta\cos\theta \tag{2}$$

The average particles' size of NCP, ZnO/NCP, TiO_2/NCP, and ZnO–TiO_2/NCP were calculated as 22, 26, 29, and 32 nm, respectively.

To have more precise particle size for ZnO–TiO_2/NCP, TEM image was recorded and as shown in Fig. 1(B) more ZnO–TiO_2/NCP particles have sizes smaller than 100 nm.

3.1.2. FT-IR results

FT-IR spectra of the parent zeolite NCP, TiO_2/NCP, and ZnO–TiO_2/NCP in the region 450–4,000 cm^{-1} are shown in Fig. 2. The spectrum (a) in Fig. 2 shows the –Si–O–Si– stretching vibrations at about 1,087 cm^{-1}, which is quite wide and overlaps with the –Al–O– and –Al–O–Si– stretching vibrations [32]. The peaks which were located at the region of 620–740 cm^{-1} are

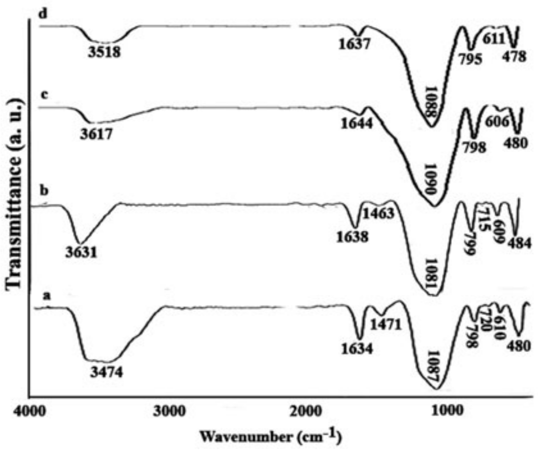

Fig. 2. FT-IR patterns (a) NCP, (b) ZnO/NCP, (c) TiO_2/NCP, (d) ZnO–TiO_2/NCP.

attributed to the stretching modes involving mainly the tetrahedral atoms. In general, the stretching modes are sensitive to the Si/Al ratio of the zeolite framework and can shift to lower frequencies with decreasing the Si/Al ratio. Another group of frequencies is sensitive to the linkages type between the secondary building units of zeolite framework that occurs in the region of 500–600 cm^{-1}. This relates to the presence of a double ring in the framework and can be observed for all zeolites containing the double four and double six rings. The bands located in the region of 1,634–1,644 and 3,474 cm^{-1} relate to the deformation mode of water and the OH stretching mode, respectively [33].

Comparison of FT-IR spectra of raw clinoptilolite and ZnO–TiO_2/NCP samples (spectra "a" and "c" in Fig. 2) shows some shifts in peaks positions (wavenumbers in parenthesis belong to ZnO–TiO_2/NCP sample) of 3,474 (3,518), 1,634 (1,637), 1,087 (1,088), 798 (795), and 610 (611) cm^{-1}. In FT-IR of modified samples, the peaks located at 720 and 1,471 cm^{-1} were also disappeared and a new peak was observed at about 478–480 cm^{-1} due to structural changes during the formation of ZnO–TiO_2 in the calcination process. In addition, for modified samples, some shifts were observed at peak position of –Si–O–Si– and Al–O–Al stretching vibrations (at about 1,087 cm^{-1}) and the peaks located at right side of this peak, showing entrance of TiO_2 and ZnO–TiO_2 onto NCP particles. These results have a good compliance with Breck's results [32].

3.1.3. DRS results

UV-vis DRS spectra of NCP, ZnO/NCP, TiO_2/NCP, and ZnO–TiO_2/NCP samples in the range of 190–900 nm were recorded and the corresponding spectra are shown in Fig. 3. The charge transfer $O_2^- \rightarrow Al^{3+}$ with participation of aluminum atoms at different locations of zeolite (surface, corners, defects, etc.) causes an absorption peak in the wavelengths lower than 350 nm. Based on the literature [34], after calcination of metal-exchanged forms of zeolites, some red shifts in the band-gap transition to longer wavelengths have observed. Such changes are present in our results, so the red shifts with together the peak broadening were observed in the absorption spectra of the modified ZnO/NCP, TiO_2/NCP, and ZnO–TiO_2/NCP samples. Also, the absorbance of the modified samples was significantly enhanced by loading sufficient amounts of the proposed semiconductors. The following trend was observed for the peak broadening and enhancement in the absorption intensity:

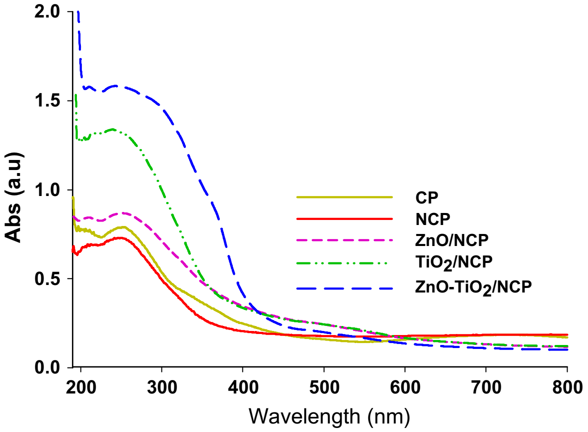

Fig. 3. DRS patterns of CP, NCP, ZnO/NCP, TiO_2/NCP, and ZnO–TiO_2/NCP.

$$\mathrm{NCP} < \mathrm{ZnO/NCP} < \mathrm{TiO_2/NCP} < \mathrm{ZnO} - \mathrm{TiO_2/NCP}$$

The results indicate that the absorption peak of the natural zeolite was enhanced in the nano-zeolite which may be attributed to the changes in the crystallite phase and reducing in the particles size. Based on the literature, absorption band at about 370 and 400 nm corresponding to the band gap width of the ZnO and TiO_2 nano-particles appears with increasing the amounts of TiO_2 and ZnO loading [35].

3.2. Photodegradation experiments

3.2.1. Effect of catalyst

Effect of different catalysts such as: ZnO/NCP, TiO_2/NCP, bulk TiO_2, and ZnO–TiO_2/NCP was studied on the degradation extent of phenol in the proposed wastewater sample. According to atomic spectroscopic determination of zinc and titanium, the metal oxides content of the used catalysts was determined and the results are collected in Table 1. The photodegradation extents of 6.5, 10.9, and 7.9% were respectively obtained in presence of ZnO/NCP, bulk TiO_2, and TiO_2/NCP during 300 min irradiation, while the hybrid ZnO–TiO_2/NCP showed about 20% degradation efficiency. The band gap energy of TiO_2 and ZnO are, respectively, about 3.2 and 3.4 eV [36]. Hence, in the hybrid ZnO–TiO_2–NCP composite, transferring of the excited electrons from ZnO conductance band to TiO_2 conduction band prevents electron-hole recombination results a considerable enhancement in the degradation efficiency. Our results agree with the literature [37,38]. According to obtained

Table 1
Abbreviations of the catalysts and their metal oxide components

Symbol of photocatalyst	meq ZnO/g	meq TiO_2/g	ZnO%	TiO_2%
ZnO/NCP	1.3	0.0	5.2	0.0
TiO_2/NCP	0.0	1.4	0.0	5.5
ZnO–TiO_2/NCP	1.2	1.4	4.7	5.5

results, the ZnO–TiO_2/NCP catalyst was used for next studies.

3.2.2. Effect of the photocatalytic dosage

In order to determine the optimum amount of the ZnO–TiO_2/NCP photocatalyst, some experiments were carried out with varying amounts of ZnO–TiO_2/NCP catalyst (from 0.05 to 0.20 g L^{-1}) and100 times diluted wastewater sample at pH 3 and the corresponding results are given in Fig. 4. The degradation rate was increased with increasing in the photocatalyst amount (to 0.1 g L^{-1}) and thereafter decreased. With increasing the photocatalyst amount, the number of available adsorption sites increases which brings the phenol molecules near the catalyst surface where hydroxyl radicals form [15,39]. However, by increasing the catalyst dose, the catalyst surface area, the light absorption, and consequently the creation of number of active species will increase which in turn increase the degradation extent of pollutants. Further increase in the weight of the catalyst showed a negative effect [40]. With increase in the photocatalyst amount, some adsorption sites are partially occupied together with the particle interaction, such as aggregation. These phenomena lead to decrease in total surface area of the photocatalyst and also an increase in diffusion path length. On the other hand, at higher doses, beyond the optimum value, some parts of the catalyst are in the dark causing a decrease in the light penetration. Deactivation of activated molecules by collision with ground state molecules and light scattering may also reduce the catalytic activity in the higher amounts of catalyst [41].

3.2.3. Effect of initial concentration of pollutant

For study of the influence of initial concentration of the wastewater sample, because of its important role on the degradation efficiency, some photodegradation experiments were done using 1, 10, 100, 500, and 1,000 times diluted wastewater sample containing 0.1 g L^{-1} of ZnO–TiO_2/NCP catalyst and pH 3. For each sample, one blank solution was selected with the same concentration and the degradation process was done, as mentioned in Section 2.3. The corresponding results collected are shown in Fig. 5.

It was observed that 100 times diluted wastewater sample was the optimum concentration for efficient degradation of wastewater. The lifetimes of hydroxyl radicals are very short (only a few nanoseconds) and thus they can only react where they form [42]. Hence, at low concentrations, less molecules and phenol can

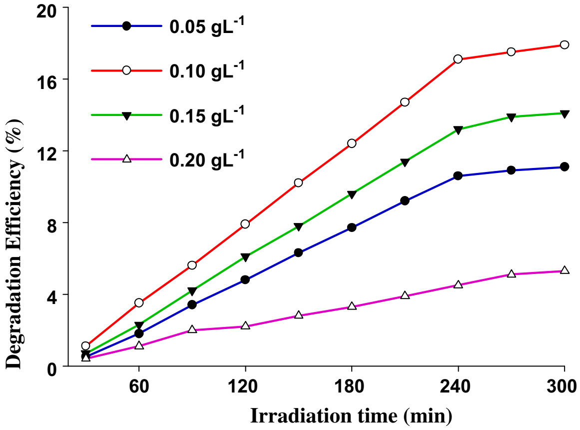

Fig. 4. Effect of photocatalyst amount on the degradation extent of phenol in 100 times diluted wastewater sample, pH 3.0 at $\lambda = 270$ nm.

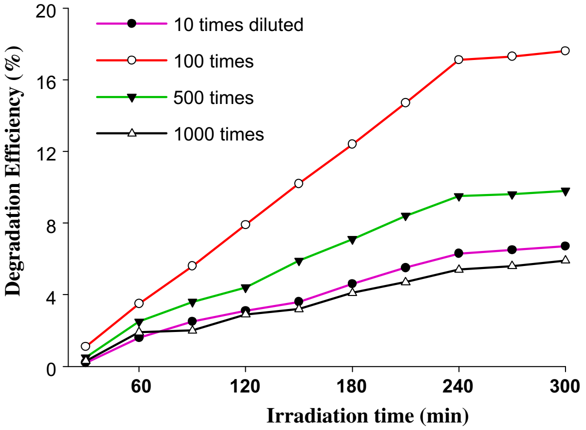

Fig. 5. Effect of pollutant concentration on the degradation extent of phenol, conditions: 0.1 g L^{-1} of catalyst and pH 3.0, $\lambda = 270$ nm.

reach near the surface of the photocatalyst, where hydroxyl radical formed. Hence, hydroxyl radicals can deactivate before reacting with molecules of phenol and hence the degradation extent decrease. With increasing in the pollutant concentration, more phenol molecules reach near the catalyst surface and easily react with hydroxyl radicals. At high concentrations, the wastewater starts acting as a filter for the incident light and it does not permit the desired light intensity to reach the semiconductor surface in a limited time domain; thus, photodegradation percent decreases [43]. In general, there are a lot of things like salts and detergents in wastewater and especially in this wastewater the concentration was very high that lead to prevention of photons reaching catalyst surface and thus the absorption of photons by the catalyst decreases. Hence, relative dilution of wastewater decreases the problems of salts and detergents and hence increases the degradation efficiency. But, high dilution of the wastewater sample decreases the probability of collision between pollutant molecules with hydroxyl radicals which lead to decrease in the degradation extent of the pollutant [43–45].

3.2.4. Effect of pH

The effect of solution pH was investigated by performing the experiments at various pH covering the range from 3 to 8, adjusting by diluted HCl or NaOH solution. The pH is one of the most important factors controlling the photocatalysis process of pollutants especially due to its effects on the charge of the catalyst surfaces [46]. The maximum photodegradation of the proposed wastewater was observed at pH 3 (Fig. 6).

Changes to protonation–deprotonation characteristics of the mineral surface due to structural transformation will alter the pH_{pzc} and therefore the equilibrium pH of the suspension [47]. The pH_{pzc} is a point at which the surface acidic (or basic) functional groups no longer contribute to the pH value of the solution [48]. According to inset of Fig. 6, the pH_{pzc} for the used ZnO–TiO_2/NCP was obtained about 6.6. At pH values smaller than pH_{pzc}, the charge of the catalyst is positive, and negative at higher values. In our idea, in pH 3, the catalyst surface has a net positive charge, and phenol molecules are partially protonated and most of phenol molecules are as non-protonated form. Hence, an attractive force brings phenol molecules near the catalyst surface. In other alternative, an attractive force can create between the positive charges of the catalyst surface and phenolic π-electrons. In both conditions, more phenol molecules can reach near the catalyst surface, where hydroxyl and superoxide radicals are present during the irradiation process. With increasing the pH to 5, the positive charge density of the catalyst surface reduces and the extent of the above-mentioned attractive force and hence the degradation extent decrease.

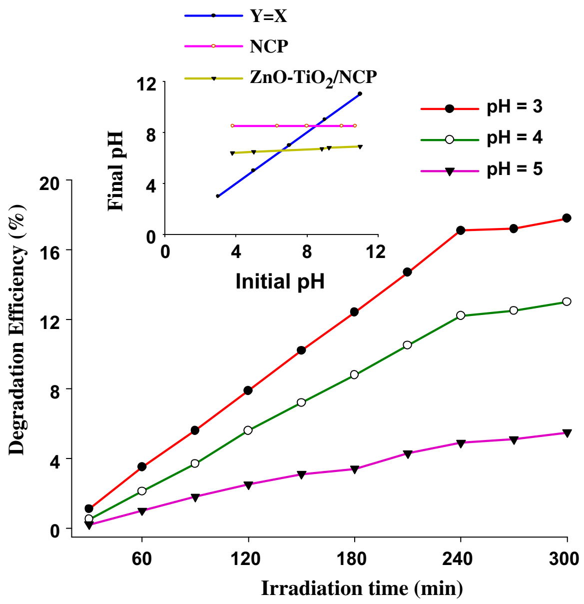

Fig. 6. Diagram of examination effect pH on the degradation of aqueous solution of the pollutant, conditions: concentration 100 times diluted and g L^{-1} of catalyst, $\lambda = 270$ nm (inset: pH_{pzc} for NCP and ZnO–TiO_2/NCP).

3.2.5. Mineralization studies

To confirm the mineralization of the proposed wastewater, photodegradation of a sample was studied under the optimized conditions (100 times diluted solution, pH 3, and 0.1 g L^{-1} of the catalyst) and the reduction of TOC was followed. Decrease in TOC extent in the samples during 0, 1, and 2 h photodegradation experiments were, respectively, found as 2,536, 2,206, and 1886 mg L^{-1}. Decrease in TOC content of the proposed wastewater during the irradiation process confirms mineralization of the sample to smaller fragments.

4. Conclusion

Results of this work confirmed that hybridization of ZnO–TiO_2 semiconductors and supporting it on clinoptilolite nano-particles can efficiently increase the photodegradation activity of the obtained ZnO–TiO_2/NCP with respect to the supported ZnO and TiO_2 alone on NCP. The efficiency of the proposed

ZnO–TiO_2/NCP catalyst was also better than bulk TiO_2. On the other hand, both zeolitic bed and hybridization of two semiconductors distribute the excited electrons thorough the catalyst and hence prevent recombination of e-hole pairs which as a desirable phenomenon in the photodegradation processes led to increase in the degradation extent.

References

[1] Y. Huang, H. Cao, Y. Lin, X. Wang, Adsorption of phenol with the crosslinked polymer of P(MMA-MAh)-PEG_{33}, Desalin. Water Treat. 51 (2013) 6755–6760.

[2] A.H. Sulaymon, D.W. Abbood, A.H. Ali, Competitive biosorption of phenol and lead from synthetic wastewater onto live and dead microorganisms, Desalin. Water Treat. 45 (2012) 331–342.

[3] H. Cherifi, F. Bentahar, S. Hanini, Biosorption of phenol by dried biomass, Desalin. Water Treat. 52 (2014) 1699–1704.

[4] J. Liu, J. Xie, Zh. Ren, W. Zhang, Solvent extraction of phenol with cumene from wastewater, Desalin. Water Treat. 51 (2013) 3826–3831.

[5] Y. Wu, G. Tian, H. Tan, X. Fu, Pervaporation of phenol wastewater with PVDF–PU blend membrane, Desalin. Water Treat. 51 (2013) 5311–5318.

[6] A.H. Mahvi, A. Maleki, Photosonochemical degradation of phenol in water, Desalin. Water Treat. 20 (2010) 197–202.

[7] A. Nezamzadeh-Ejhieh, Z. Salimi, Heterogeneous photodegradation catalysis of o-phenylenediamine using CuO/X zeolite, Appl. Catal., A 390 (2010) 110–118.

[8] A. Nezamzadeh-Ejhieh, M. Amiri, CuO supported clinoptilolite towards solar photocatalytic degradation of p-aminophenol, Powder Technol. 235 (2013) 279–288.

[9] A. Nezamzadeh-Ejhieh, S. Khorsandi, Photocatalytic degradation of 4-nitrophenol with ZnO supported nano-clinoptilolite zeolite, J. Ind. Eng. Chem. 20 (2014) 937–946. Available from: http://dx.doi.org/10.1016/j.jiec.2013.06.026.

[10] A. Nezamzadeh-Ejhieh, M. Karimi-Shamsabadi, Decolorization of a binary azo dyes mixture using CuO incorporated nanozeolite-X as a heterogeneous catalyst and solar irradiation, Chem. Eng. J. 228 (2013) 631–641.

[11] Ch.-Y. Kuo, Ch.-H. Wu, Sh.-T. Chen, Decolorization of C.I. reactive red 2 by UV/TiO_2/PAC and visible light/TiO_2/PAC systems, Desalin. Water Treat. 52 (2014) 834–843.

[12] J.K. Yang, S.M. Lee, M. Farrokhi, O. Giahi, M. Shirzad Siboni, Photocatalytic removal of Cr(VI) with illuminated TiO_2, Desalin. Water Treat. 46 (2012) 375–380.

[13] A. Nezamzadeh-Ejhieh, F. Khodabakhshi-Chermahini, Incorporated ZnO onto nano clinoptilolite particles as the active centers in the photodegradation of phenylhydrazine, J. Indust. Eng. Chem. 20 (2014) 695–704.

[14] M.R. Samarghandi, J.K. Yang, S.M. Lee, O. Giahi, M. Shirzad-Siboni, Effect of different type of organic compounds on the photocatalytic reduction of Cr(VI) in presence of ZnO nanoparticles, Desalin. Water Treat. 52 (2014) 1531–1538.

[15] A. Nezamzadeh-Ejhieh, N. Moazzeni, Sunlight photodecolorization of a mixture of methyl orange and bromocresol green by CuS incorporated in a clinoptilolite zeolite as a heterogeneous catalyst, J. Indust. Eng. Chem. 19 (2013) 1433–1442.

[16] R.M. Mohamed, E.S. Aazam, Enhancement of photocatalytic activity of ZnO–SiO_2 by nano-sized Ag for visible photocatalytic reduction of Hg(II), Desalin. Water Treat. 50 (2012) 140–146.

[17] A. Nezamzadeh-Ejhieh, Z. Banan, Kinetic investigation of photocatalytic degradation of dimethyldisulfide by zeolite Acontaining nano CdS, Iran. J. Catal. 2(2) (2012) 77–81.

[18] N. Roostaei, F. Tezel, Removal of phenol from aqueous solutions by adsorption, J. Environ. Manage. 70 (2004) 157–164.

[19] H.R. Pouretedal, H. Motamedi, A. Amiri, Aromatic compounds photodegradation catalyzed by ZnS and CdS nanoparticles, Desalin. Water Treat. 44 (2002) 92–99.

[20] M. Pimentel, N. Oturan, M. Dezotti, M.A. Oturan, Phenol degradation by advanced electrochemical oxidation process electro-Fenton using a carbon felt cathode, Appl. Catal., B 83 (2008) 140–149.

[21] U.I. Gaya, A.H. Abdullah, Heterogeneous photocatalytic degradation of organic contaminants over titanium dioxide: A review of fundamentals, progress and problems, J. Photochem. Photobiol., C 9 (2008) 1–12.

[22] A. Nezamzadeh-Ejhieh, Z. Banan, Photodegradation of dimethyldisulfide by heterogeneous catalysis using nanoCdS and nanoCdO embedded on the zeolite A synthesized from waste porcelain, Desalin Water Treat. 52 (2014) 3328–3337. doi: 10.1080/19443994.2013.797627.

[23] A. Dhir, N.T. Prakash, D. Sud, Comparative studies on TiO_2/ZnO photocatalyzed degradation of 4-chlorocatechol and bleach mill effluents, Desalin. Water Treat. 46 (2012) 196–204.

[24] P. Pengthamkeerati, T. Satapanajaru, O. Singchan, Sorption of reactive dye from aqueous solution on biomass fly ash, J. Hazard. Mater. 153 (2008) 1149–1156.

[25] O. Korkuna, R. Leboda, J. Skubiszewska, T. Vrublevs'ka, V. Gun'ko, J. Ryczkowski, Structural and physicochemical properties of natural zeolites: Clinoptilolite and mordenite, Microporous Mesoporous Mater. 87 (2006) 243–254.

[26] F. Li, Y. Jiang, L. Yu, Z. Yang, T. Hou, S. Sun, Surface effect of natural zeolite (clinoptilolite) on the photocatalytic activity of TiO_2, Appl. Surf. Sci. 252 (2005) 1410–1416.

[27] Z. Zainal, L.K. Hui, M.Z. Hussein, A.H. Abdullah, I.R. Hamadneh, Characterization of TiO_2-chitosan/glass photocatalyst for the removal of a monoazo dye via photodegradation–adsorption process, J. Hazard. Mater. 164 (2009) 138–145.

[28] A. Charkhi, H. Kazemian, M. Kazemeini, Optimized experimental design for natural clinoptilolite zeolite ball milling to produce nano powders, Powder Technol. 203 (2010) 389–396.

[29] S. Yaşyerli, İ. Ar, G. Doğu, T. Doğu, Removal of hydrogen sulfide by clinoptilolite in a fixed bed adsorber, Chem. Eng. Process. 41 (2002) 785–792.

[30] A. Irzh, I. Genish, L. Klein, L.A. Solovyov, A. Gedanken, Synthesis of ZnO and Zn nanoparticles in microwave plasma and their deposition on glass slides, Langmuir 26(8) (2010) 5976–5984.

[31] A. Nezamzadeh-Ejhieh, Sh. Hushmandrad, Solar photodecolorization of methylene blue by CuO/X zeolite as a heterogeneous catalyst, Appl. Catal., A 388 (2010) 149–159.

[32] D.W. Breck, Zeolite Molecular Sieves: Structure, Chemistry and Uses, Wiley, New York, NY, 1974.

[33] M. Brazlauskas, S. Kitrys, Synthesis and properties of CuO/Zeolite sandwich type adsorbent-catalysts, Chin. J. Catal. 29 (2008) 25–30.

[34] I. Rodríguez Iznaga, V. Petranovskii, G. Rodríguez Fuentes, C. Mendoza, A. Benítez Aguilar, Exchange and reduction of Cu^{2+} ions in clinoptilolite, J. Colloid Interface Sci. 316 (2007) 877–886.

[35] R. Amadelli, L. Samiolo, A. Maldotti, A. Molinari, M. Valigi, D. Gazzoli, Preparation, characterization, and photocatalytic behavior of Co–TiO_2 with visible light response, Int. J. Photoenergy 2008 (2008) 1–9.

[36] R.S. Mane, W.J. Lee, H.M. Pathan, A.-H. Han, Nanocrystalline TiO_2/ZnO thin films: fabrication and application to dye-sensitized solar cells, J. Phys. Chem. B 109 (2005) 24254–24259.

[37] I. Bedja, P.V. Kamat, Capped semiconductor colloids. Synthesis and photoelectrochemical behavior of TiO_2 capped SnO_2 nanocrystallites, J. Phys. Chem. 99 (1995) 9182–9188.

[38] P. Bansal, N. Bhullar, D. Sud, Studies on photodegradation of malachite green using TiO_2/ZnO photocatalyst, Desalin. Water Treat. 12 (2009) 108–113.

[39] J.M. Herrmann, Heterogeneous photocatalysis: Fundamentals and applications to the removal of various types of aqueous pollutants, Catal. Today 53 (1999) 115–129.

[40] M. Hamity, R.H. Lema, C.A. Suchetti, H.E. Gsponer, UV–vis photodegradation of dyes in the presence of colloidal Q-CdS, J. Photochem. Photobiol., A 200 (2008) 445–450.

[41] H.R. Pouretedal, S. Sabzevari, Photodegradation study of congo red, methyl orange, methyl red and methylene blue under simulated solar irradiation catalyzed by ZnS/CdS nanocomposite, Desalin. Water Treat. 28 (2011) 247–254.

[42] R. Qadeer, A study of the adsorption of phenol by activated carbon from aqueous solutions, Turk. J. Chem. 26 (2002) 357–361.

[43] S. Akhtar, A.A. Khan, Q. Husain, Potential of immobilized bitter gourd (*Momordica charantia*) peroxidases in the decolorization and removal of textile dyes from polluted wastewater and dyeing effluent, Chemosphere 60 (2005) 291–301.

[44] M. El-Kemary, Y. Abdel-Moneam, M. Madkour, I. El-Mehasseb, Enhanced photocatalytic degradation of Safranin-O by heterogeneous nanoparticles for environmental applications, J. Lumin. 131 (2011) 570–576.

[45] A. Nezamzadeh-Ejhieh, M. Khorsandi, A comparison between the heterogeneous photodecolorization of an azo dye using Ni/P zeolite and NiS/P zeolite catalysts, Iran. J. Catal. 1(2) (2011) 99–104.

[46] M. Guedes, J.A. Ferreira, A. Ferro, pH-dependent surface charging and points of zero charge. IV. Update and new approach, Colloid Interface Sci. 337 (2009) 439–448.

[47] K.J. Reddy, Z. Zhang, M. Blaylock, Method for detecting selenium speciation in groundwater, Environ. Sci. Technol. 29 (1995) 1754–1759.

[48] F.A. Banat, B. Al-Bashir, S. Al-Asheh, O. Hayajneh, Adsorption of phenol by bentonite, Environ. Pollut. 107 (2000) 391–398.